

Burr formation in milling cross-connected microchannels with a thin slotting cutter

Yong Tang^a, Zhanshu He^{a,b,*}, Longsheng Lu^a, Hui Wang^a, Minqiang Pan^a

^a Key Laboratory of Surface Functional Structure Manufacturing of Guangdong Higher Education Institutes, South China University of Technology, 381, Wushan Road, Tianhe District, Guangzhou 510640, PR China

^b Computer-Aided Manufacturing Laboratory, Worcester Polytechnic Institute, Worcester, MA 01609, United States

ARTICLE INFO

Article history:

Received 21 March 2010

Received in revised form 7 August 2010

Accepted 18 August 2010

Available online 26 August 2010

Keywords:

Burr formation

Milling

Microchannel

Slotting cutter

ABSTRACT

This paper studies the burr formation mechanism in milling cross-connected microchannels, and investigates the influences of radial depth of cut a_e , cutting speed v , feed speed v_f and mesh size on the burr formation. A thin slotting cutter is carried out to fabricate cross-connected microchannels in a metal plate of thickness H . Two kinds of large burrs are produced in the meshes formed by two sets of perpendicular and cross-connected microchannels: flake-like burr and curl-like burr. Results indicate that when a_e is equal to or slightly larger than $H/2$, flake-like burrs are formed. When a_e is much larger than $H/2$, curl-like burrs are produced. Furthermore, curl-like burrs formed at low v are relatively longer than those formed at high v . High v_f is unfavorable for the occurrence of long curl-like burrs. In addition, larger mesh is in favor of longer burrs due to its larger capacity.

© 2010 Elsevier Inc. All rights reserved.

1. Introduction

Cross-connected microchannels (as shown in Fig. 1) are a structure with two sets of perpendicular microchannels on both sides of a plate, which intersect each other so as to form lots of meshes. Due to the existence of the meshes cross-connected microchannels are favorable for nucleation and bubbles to escape. Moreover, since microchannel has characteristic dimensions of the order of hundreds of microns, cross-connected microchannels have a larger surface area compared with original structures. Thus, cross-connected microchannels have been studied extensively [1–7] and used in thermosyphon, loop heat pipes and other two-phase cooling devices. Nowadays, methods for fabricating cross-connected microchannels mainly include photolithography, wet etching, saw dicing and wire electro-discharge machining. But all these methods are either costly or complex.

In the present work, cross-connected microchannels are fabricated with a thin slotting cutter, as shown in Fig. 1. In one of the authors' previous papers [8], this method was employed to fabricate multiple parallel microchannels simultaneously through stacking several slotting cutters together. During the machining process many burrs occur not only on both top sides of microchannels, but also in nearly every mesh. Actually, burrs on microchannels may cause several problems, such as damaging the dimensional accuracy and surface finish; reducing cutting perfor-

mance and tool life; interfering with fluid flow, increasing the cost and time of production due to deburring [9–11]. Therefore, it is necessary to study the burr formation in milling cross-connected microchannels for minimizing the burrs or even eliminating them.

According to Aurich et al. [12], in most cases burrs are defined as undesirable or unwanted projections of the material formed as the result of the plastic flow from cutting and shearing operations. Gillespie and Blotter [13] defined four basic types of burrs: Poisson, rollover and tear burrs shown in Fig. 2, and cut-off burrs. Burrs from milling operations are described as follows. Hashimura et al. [14] classified burrs in face milling as exit burr, side burr and top burr according to burr locations, burr shapes and burr formation mechanisms (as shown in Fig. 3). Nakayama and Arai [15] described machining burrs formed in various cutting operations by the combination of two systems of classification: (1) by cutting edge which is directly related to burr formation and (2) by the mode and direction of burr formation. Fig. 4 shows some types of milling burrs classified by the combination of the two systems.

Nowadays, much research has been focused on burr formation in face milling. Chern [9] studied the burr formation mechanisms in face milling process and investigated the influence of cutting conditions on burr formation in face milling of aluminum alloys. Five types of burrs were observed in the experiments: knife-type, wave-type burr, curl-type, edge breakout and secondary burr. Silva et al. [11] studied the burr behaviour during face milling of motor engine blocks. The burr was mainly dependent on the maximum flank wear and on the exit angle of the milling cutter from the workpiece. Chu and Dornfeld [16] proposed a set of geometric algorithms for avoiding tool exits in planar milling. Experimental results showed that

* Corresponding author. Tel.: +86 13570586957; fax: +86 020 87114634.
E-mail addresses: hezhangshu@qq.com, hezhangshu2004@126.com (Z. He).

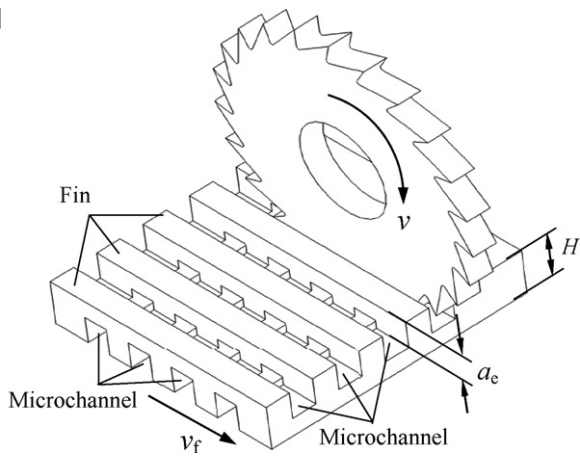


Fig. 1. Schematic diagram of milling cross-connected microchannels with a thin slotting cutter.

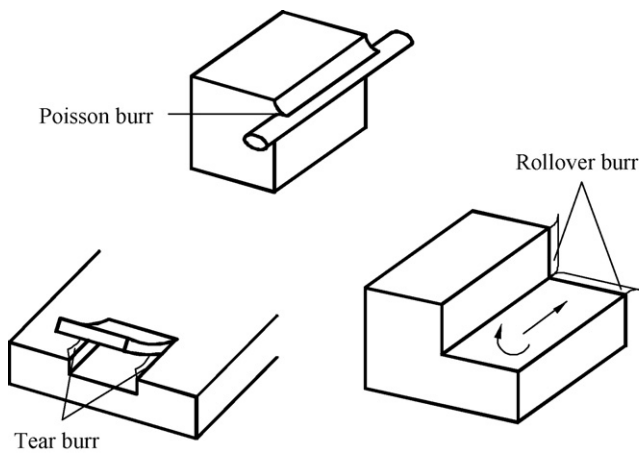


Fig. 2. Schematic diagram of Poisson, tear and rollover burr [13].

only entrance burrs could occur by using the proposed methods, which were usually considered burr-free. Lin [17] investigated burr formation and tool chipping during the face milling of stainless steel by using a fly milling cutter. Five different types of burr were produced on the exit edge, e.g. knife-type, saw-type, burr breakage curl-type and wave-type. However, until now little research has

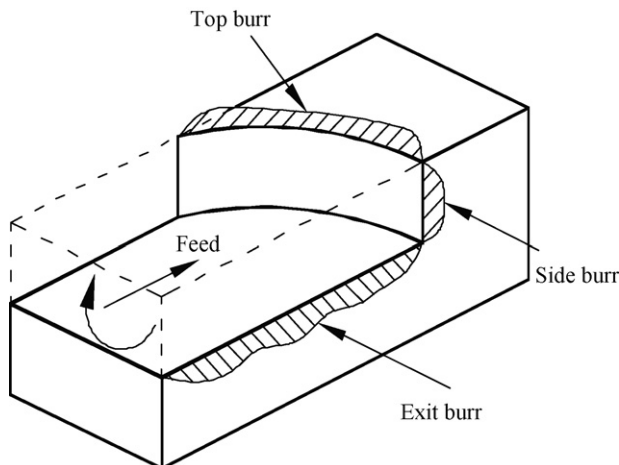


Fig. 3. Types of milling burrs classified by burr locations, burr shapes and burr formation mechanisms [14].

(1) Cutting edge directly concerned	Initials
Major cutting edge	M
Corner or minor cutting edge	C
(2) Direction of burr formation	Initials
Backward flow	B
Sideward flow	S
Forward flow	F

(a) Cutting edge and direction of burr formation and their initials

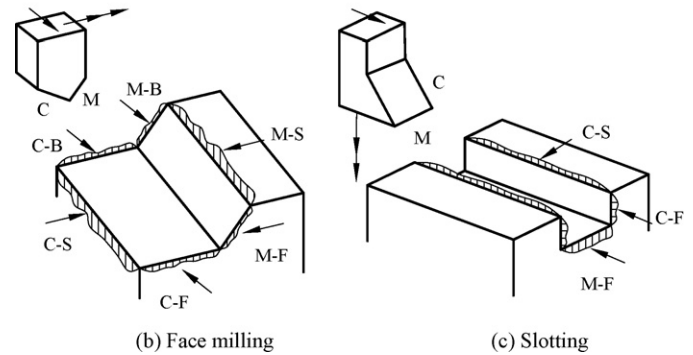


Fig. 4. Types of milling burrs classified by cutting edge and by the mode and direction of burr formation [15].

been carried out on burr formation in slotting. Therefore, in this paper the burr formation mechanism in milling cross-connected microchannels with a thin slotting cutter are presented. In addition, the influences of cutting parameters and mesh size on burr formation are analyzed.

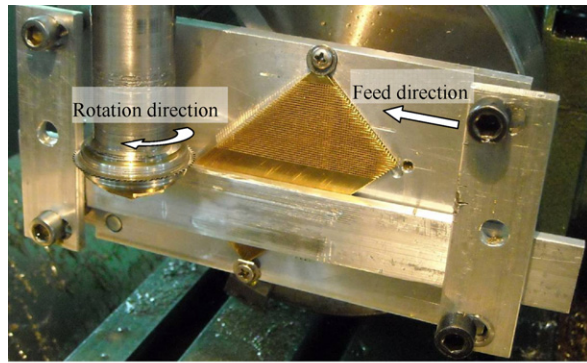
2. Experimental

The experiments are conducted on a vertical milling machine X5032 from Tengzhou Xili Machine Tool Co., Ltd., China, as shown in Fig. 5(a). The tool used is a slotting cutter (Fig. 5(b)) made of high-speed steel W₁₈Cr₄V with a diameter of 40 mm. The slotting cutter has 72 teeth and the tooth depth is 1 mm. Rake angle and clearance angle is 5° and 16°, respectively. The thickness of the slotting cutter is chosen according to the required microchannel width. The cutting edge radius r_e is a few microns. A rectangular metal plate is chosen as the workpiece made of brass CuZn37 with dimensions of 70 mm × 40 mm × 2 mm. The workpiece is located on a special fixture and pressed tightly by another long metal plate, while the special fixture is mounted on a three jaw chuck. Then, microchannels in any direction can be fabricated through rotating the chuck by adjusting the index head. During the machining process, the slotting cutter rotates with the spindle speed n (cutting speed v) and the workpiece moves with the feed speed v_f . Equally spaced teeth of the slotting cutter enter the workpiece in up milling. One set of microchannels is fabricated on the one side of the brass plate, and then another set of microchannels, which is perpendicular to the first set of microchannels, is fabricated on the other side. Two sets of microchannels have the same depth, and they intersect each other to form a mesh (as shown in Fig. 5(c)). Surface morphologies of cross-connected microchannels are observed by a scanning electron microscope S-520 from Hitachi.

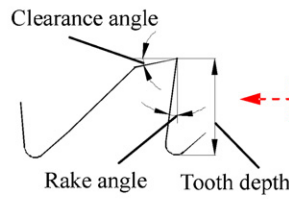
The undeformed chip thickness a_c (Fig. 6) can be approximated as:

$$a_c = f_z \sin \psi = \frac{v_f \sin \psi}{Nn} \quad (1)$$

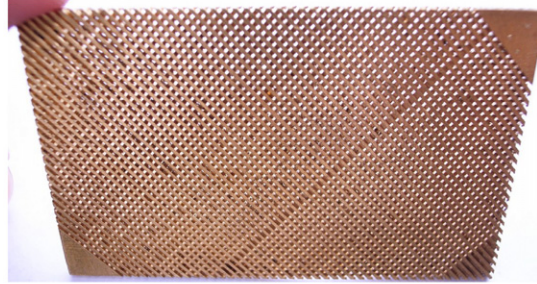
where f_z is the feed per tooth, N is the number of teeth on the cutter and ψ is a random angle between 0 and θ shown in Fig. 6.



(a) In situ process of milling cross-connected microchannels



(b) Slotting cutter



(c) Cross-connected microchannel mesh plate

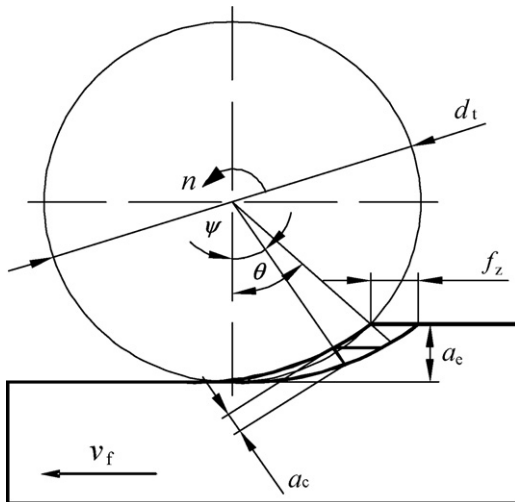
Fig. 5. Fabrication of cross-connected microchannels with a slotting cutter.

The undeformed chip thickness increases from zero to the maximum undeformed chip thickness a_{cmax} with every pass of a tooth. a_{cmax} occurs when a tooth enters the uncut surface and can be calculated by [18]:

$$a_{cmax} = f_z \sin \theta = \frac{2v_f}{Nn} \sqrt{\frac{a_e}{d_t} \left(1 - \frac{a_e}{d_t}\right)} \quad (2)$$

where θ is the angle of immersion, which is also the maximum value of ψ , d_t is the diameter of the slotting cutter, and a_e is the radial depth of cut.

Cutting parameters in the present experiments are described in Table 1. After calculation it is found that a_{cmax} is always smaller than $10 \mu\text{m}$, which is of the same order of magnitude as the cutting edge radius. Thus, the effect of the cutting edge radius cannot be ignored.

**Fig. 6.** Geometry of milling operation.

3. Results and discussion

In the milling process, every tooth cuts into the workpiece from the bottom of a microchannel and exits at the top. When the tool is leaving the material, some tear burrs occur on both top sides of the microchannel as the result of material tearing off the workpiece rather than shearing. Furthermore, when fabricating the second set of microchannels, burrs occur in nearly every mesh. As shown in Fig. 7, the burrs in the meshes are much larger than the top burrs. Hence, in the following sections much research is focused on the burrs in the meshes. In these experiments two kind of burrs, flake-like burrs and curl-like burrs, are observed in the meshes. Next, the formation mechanism of the two kinds of burrs is presented. In addition, the influences of cutting parameters and mesh size on burr formation are analyzed.

3.1. Burr formation mechanism

3.1.1. Relationship between chip formation and the minimum chip thickness h_m

Since the cutting edge radius r_e is of the same order of magnitude as the undeformed chip thickness a_c , the effective rake angle γ becomes highly negative, which induces the machining process to change from a shearing-dominated process to a ploughing-dominated process [19–22]. As shown in Fig. 8(a), When $a_c < h_m$, only elastic–plastic deformation occurs and chips will not be formed until a_c accumulates and surpasses h_m . The elastic deformation recovers after the tool has passed. When $a_c = h_m$, chips are

Table 1
Cutting parameters in the present experiments.

Cutting speed v (m/min)	Feed speed v_f (mm/min)	Radial depth of cut a_e (mm)
29.5 ($n = 235$ r/min)	37.5	0.95
59.7 ($n = 475$ r/min)	75	1
119.4 ($n = 950$ r/min)	150	1.2

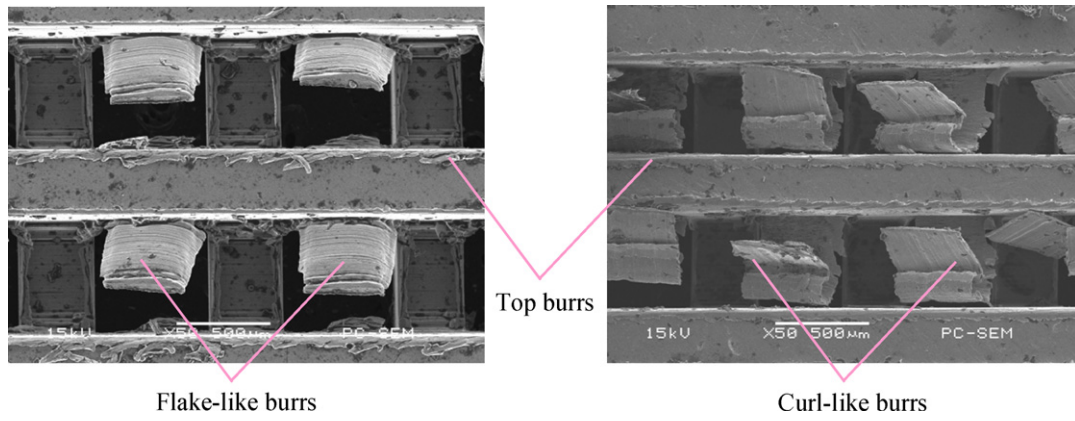


Fig. 7. Burrs produced in the process of milling cross-connected microchannels.

initially formed with some elastic–plastic deformation still occurring, as illustrated in Fig. 8(b). As a result, the removed depth of the workpiece is less than the desired depth. When $a_c > h_m$, the elastic–plastic deformation decreases dramatically and almost all the undeformed chip thickness is removed as a chip, as depicted in Fig. 8(c).

3.1.2. Formation mechanism of flake-like burrs

Since two sets of microchannels on both sides of the metal plate are in the same depth, in theory they will intersect each other so as to form lots of meshes when the radial depth of cut a_e is equal to or larger than half of the metal plate thickness $H/2$. However, due to the elastic deformation the removed depth of the workpiece

is actually less than the desired depth. So when a_e is equal to or slightly larger than $H/2$, a thin layer of metal still exists between two sets of perpendicular microchannels. During the machining process the thin layer of metal becomes fractured under the compression of the tool so as to form flake-like burrs, as shown in Fig. 9. No flake-like burr occurs when a_e is much larger than $H/2$.

3.1.3. Formation mechanism of curl-like burrs

In the milling process, a chip may not be formed with every pass of a tooth, especially when a_c is much smaller than the cutting edge radius. Due to the ploughing effect, metal in the fins generates plastic deformation and then accumulates, leading to an increase of a_c . After a few passes, a_c will surpass h_m and then be removed as a chip. So the machining process may change from a ploughing-dominated process to a shearing-dominated process and back again to a ploughing-dominated process. However, when

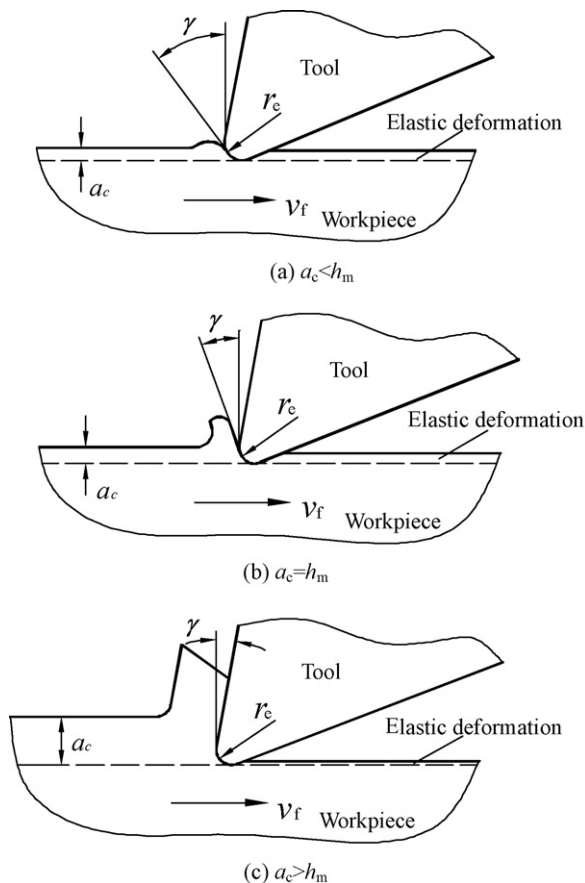


Fig. 8. Effect of the minimum chip thickness h_m on chip formation [19–22].

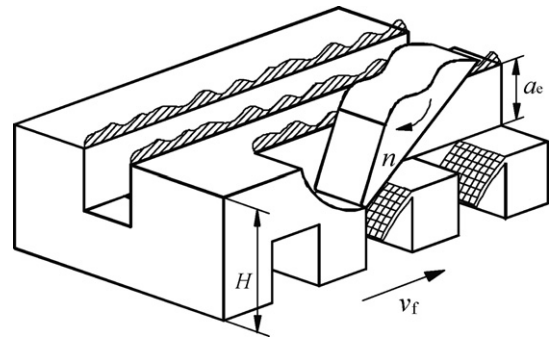


Fig. 9. Schematic diagram of the formation mechanism of flake-like burrs.

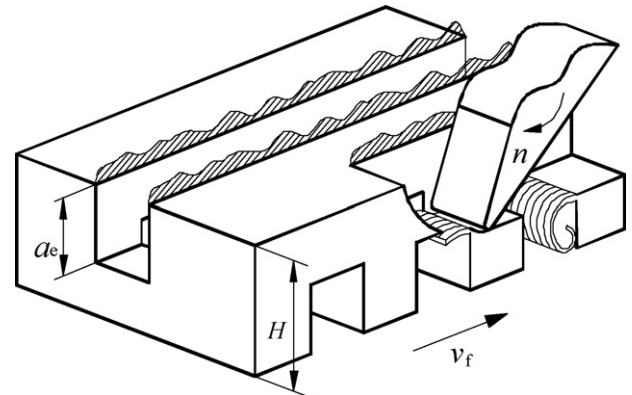


Fig. 10. Schematic diagram of the formation mechanism of curl-like burrs.

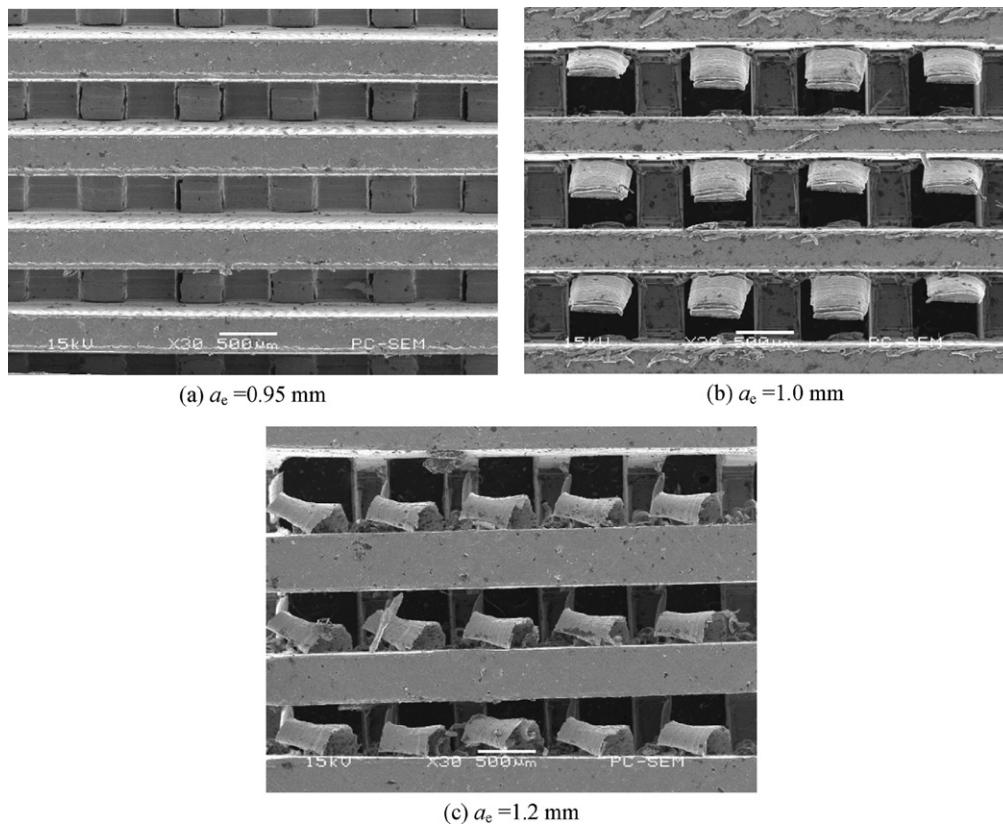


Fig. 11. Burrs formed at different radial depths of cut a_e ($v = 29.5$ m/min ($n = 235$ r/min), $v_f = 37.5$ mm/min).

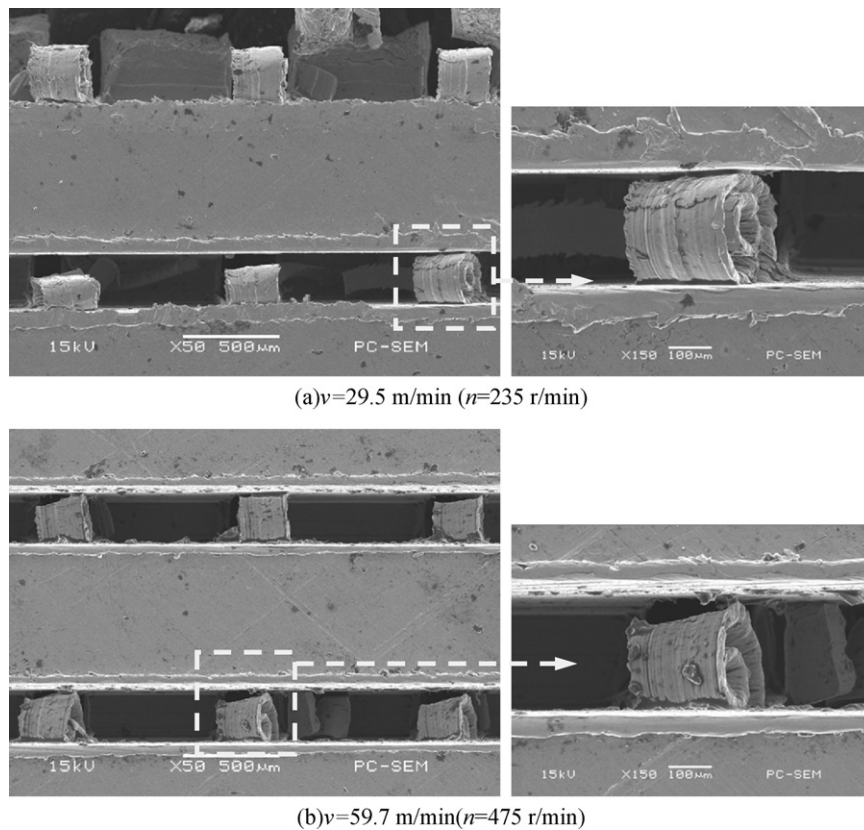


Fig. 12. Curl-like burrs formed at different cutting speeds v ($v_f = 37.5$ mm/min, $a_e = 1.2$ mm).

a_e is much larger than $H/2$, lots of meshes are formed. Due to the existence of the meshes a small part of metal in the fins will not accumulate but flow into the meshes successively with more teeth passing, as shown in Fig. 10. The metal rolls over seriously and forms curl-like burrs due to the successive compression of many passing teeth and the obstacle of the side face of the microchannel in front.

3.2. Effects of cutting parameters and mesh size on burr formation

From Fig. 7 it can be seen that the burr width is approximately equal to the microchannel width, which is determined by the thickness of the slotting cutter. Furthermore, radial depth of cut a_e , cutting speed v , feed speed v_f and mesh size also have great effects on burr formation. The effects are discussed in detail below.

3.2.1. Radial depth of cut a_e

Burrs formed at different radial depths of cut a_e are shown in Fig. 11. No mesh is formed when a_e is 0.95 mm, which is slightly smaller than $H/2$. This is because a relatively thick layer of metal still exists between two sets of perpendicular microchannels. It can be seen that the thick layer of metal becomes slightly fractured under the compression of the tool. When a_e is 1 mm, as mentioned above, flake-like burrs occur in every mesh. Under the compression of the tool the flake-like burrs become relatively seriously deformed, leading to many shallow linear textures on the burr surface opposite to the rake face. When a_e is 1.2 mm, no flake-like burrs but curl-like burrs occur in every mesh. The curl-like burrs usually roll over seriously. The curl-like burrs produced in the same machining conditions have almost the same curling direction and degree.

To ensure that any two perpendicular microchannels are cross-connected and then a mesh can be formed, a_e is usually chosen to be much larger than $H/2$. In this condition, only curl-like burrs occur in every mesh. Therefore, research in the following sections is focused on curl-like burrs.

3.2.2. Cutting speed v

Curl-like burrs formed at different cutting speeds v are shown in Fig. 12. Curl-like burrs formed at low cutting speed are relatively longer and thinner than those formed at high cutting speed. When machining at low cutting speed, metal in the fins has relatively sufficient time for plastic deformation and then flows into the meshes. On the contrary, insufficient time is provided for plastic deformation when machining at high cutting speed, so most of metal in the fins accumulates quickly and then be removed, and only little material flows into the meshes. Thus, curl-like burrs formed at high cutting speed are relatively short, and due to slight plastic deformation, they are relatively thick. From this it can be seen that plastic deformation has a great impact on burr formation in milling process. In addition, because of serious ploughing and rubbing when many teeth pass successively, some heat is produced, especially when machining at high cutting speed. As a result, a small part of metal on the surface of curl-like burrs melts and finally sticks to the side faces of the microchannels.

3.2.3. Feed speed v_f

Curl-like burrs formed at different feed speeds v_f are shown in Figs. 12(b) and 13. Because the plastic deformation decreases as the feed speed increases and slight plastic deformation is unfavorable

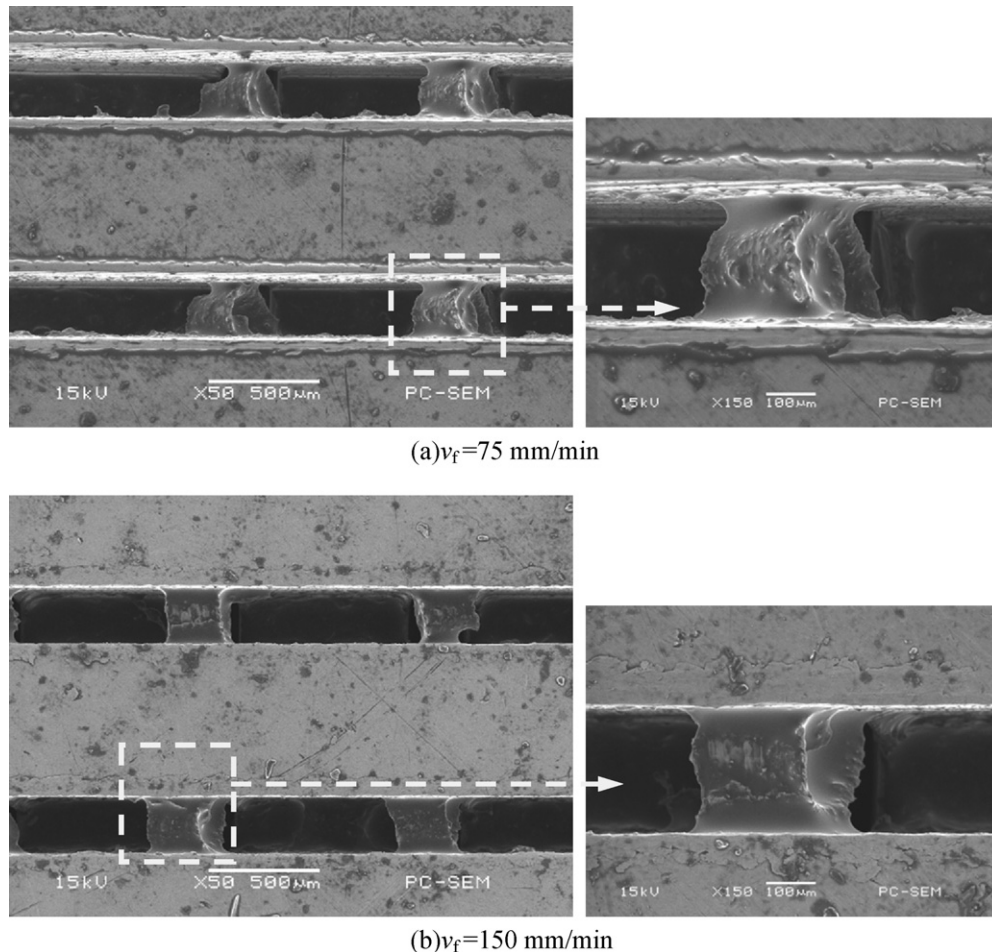


Fig. 13. Curl-like burrs formed at different feed speeds v_f ($v = 59.7$ m/min ($n = 475$ r/min), $a_e = 1.2$ mm).

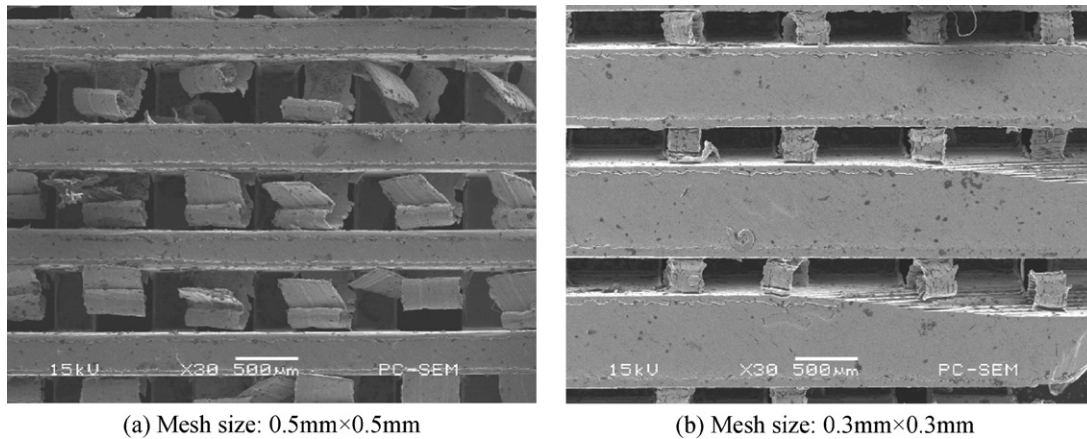


Fig. 14. Relationship between curl-like burr formation and mesh size ($a_e = 1.2$ mm, $v = 29.5$ m/min ($n = 235$ r/min), $v_f = 75$ mm/min).

for the occurrence of long curl-like burrs, curl-like burrs formed at low feed speed are longer than those formed at high feed speed. In addition, more heat is produced as the feed speed increases, so metal on the surface of curl-like burrs melts seriously and finally sticks tightly to the side faces of the microchannels.

3.2.4. Mesh size

As mentioned above, metal in the fins flows into the meshes successively and forms curl-like burrs. So the burr formation is related to the mesh, which is a square with its side length equal to the microchannel width. As shown in Fig. 14, larger mesh size is in favor of longer burrs. This is because larger meshes can hold more metal, and metal in the fins can flow into large meshes more easily than into small meshes. Although curl-like burrs originate from metal in the fins, their lengths do not increase with the increase of the fin width. So it can be concluded that only a small part of metal in the fins flows into the meshes and the metal volume is not influenced by the fin width but by the mesh size. Moreover, curl-like burrs may be longer than the fin width, and this cannot happen when one tooth passes. So it is demonstrated that curl-like burrs are formed not suddenly with one tooth pass but successively with many teeth passing. In addition, almost all the curl-like burrs turn back after they are blocked by the side face of the microchannel in front, which makes burrs roll over seriously. The more seriously the curl-like burrs roll over, the rougher their surfaces become.

4. Conclusions

In this paper, a thin slotting cutter is used for fabricating cross-connected microchannels in a metal plate with a thickness H . The burr formation mechanism in milling cross-connected microchannels is studied. The influences of radial depth of cut a_e , cutting speed v , feed speed v_f and mesh size on burr formation are investigated. The most important experimental results are as follows:

- (1) Two kinds of large burrs are produced in the meshes formed by the two sets of perpendicular and cross-connected microchannels: flake-like burr and curl-like burr. When a_e is equal to or slightly larger than $H/2$, a thin layer of metal still exists between two sets of perpendicular microchannels and becomes fractured so as to form flake-like burrs. When a_e is much larger than $H/2$, with many teeth passing, a small part of metal flows successively into the meshes and rolls over so as to form curl-like burrs.
- (2) Plastic deformation has a great impact on the formation of curl-like burrs in the milling process. Since possessing sufficient time for plastic deformation, curl-like burrs formed at low v

are relatively longer than those formed at high v . As the plastic deformation decreases with the increase of v_f , high v_f is unfavorable for the occurrence of long curl-like burrs.

- (3) A larger mesh size favors the formation of longer burrs due to its larger capacity.

Acknowledgements

The present research is financially supported by the National Natural Science Foundation of China (Nos. 50930005, 50805052), the Joint Funds of NSFC-Guangdong of China under Grant (No. U0834002), Guangdong Province Natural Science Foundation (No. 07118064) and the China Scholarship Council.

References

- [1] Launay S, Fedorov AG, Joshi Y, Cao A, Ajayan PM. Hybrid micro-nano structured thermal interfaces for pool boiling heat transfer enhancement. *Microelectron J* 2006;37:1158–64.
- [2] Murthy S, Joshi Y, Gurram S, Nakayama W. Enhanced boiling heat transfer simulation from structured surfaces: semi-analytical model. *Int J Heat Mass Transf* 2006;49:1885–95.
- [3] Ghiu CD, Joshi YK. Visualization study of pool boiling from thin confined enhanced structures. *Int J Heat Mass Transf* 2005;48:4287–99.
- [4] Ghiu CD, Joshi YK. Boiling performance of single-layered enhanced structures. *J Heat Transf (Trans ASME)* 2005;127:675–83.
- [5] Ramaswamy C, Joshi Y, Nakayama W, Johnson WB. High-speed visualization of boiling from an enhanced structure. *Int J Heat Mass Transf* 2002;45:4761–71.
- [6] Ramaswamy C, Joshi Y, Nakayama W, Johnson WB. Effects of varying geometrical parameters on boiling from microfabricated enhanced structures. *J Heat Transf (Trans ASME)* 2003;125:103–9.
- [7] Ramaswamy C, Joshi Y, Nakayama W, Johnson WB. Semi-analytical model for boiling from enhanced structures. *Int J Heat Mass Transf* 2003;46:4257–69.
- [8] Pan MQ, Zeng DH, Tang Y. Feasibility investigations on multi-cutter milling process: a novel fabrication method for microreactors with multiple microchannels. *J Power Sources* 2009;192:562–72.
- [9] Chern GL. Experimental observation and analysis of burr formation mechanisms in face milling of aluminum alloys. *Int J Mach Tools Manuf* 2006;46:1517–25.
- [10] Ballou JR, Joshi SS, DeVor RE, Kapoor SG. Burr formation in drilling intersecting holes with Machinable Austempered Ductile Iron (MADITM). *J Manuf Process* 2007;9:35–46.
- [11] Silva LCD, Melo ACAD, Machado AR, Silva MBD, Junior AMS. Application of factorial design for studying the burr behaviour during face milling of motor engine blocks. *J Mater Process Technol* 2006;179:154–60.
- [12] Aurich JC, Dornfeld D, Arrazola PJ, Franke V, Leitz L, Min S. Burrs-analysis, control and removal. *CIRP Ann Manuf Technol* 2009;58:519–42.
- [13] Gillespie LK, Blotter PT. The formation and properties of machining burrs. *ASME J Eng Ind* 1976;98:66–74.
- [14] Hashimura M, Hassamont J, Dornfeld DA. Effect of in-plane exit angle and rake angles on burr height and thickness in face milling operation. *J Manuf Sci Eng (Trans ASME)* 1999;121:13–9.
- [15] Nakayama K, Arai M. Burr formation in metal cutting. *CIRP Ann* 1987;36:33–6.

- [16] Chu CH, Dornfeld D. Geometric approaches for reducing burr formation in planar milling by avoiding tool exits. *J Manuf Process* 2005;7:182–95.
- [17] Lin TR. Experimental study of burr formation and tool chipping in the face milling of stainless steel. *J Mater Process Technol* 2000;108:12–20.
- [18] Zeng ZX, Lv M, Ya G, Liu WY. *Fundamentals of machine manufacturing technology*. Wuhan: Wuhan University of Technology Press; 2007.
- [19] Aramcharoen A, Mativenga PT. Size effect and tool geometry in micromilling of tool steel. *Precis Eng* 2009;33:402–7.
- [20] Lee K, Dornfeld DA. Micro-burr formation and minimization through process control. *Precis Eng* 2005;29:246–52.
- [21] Schaller T, Bohn L, Mayer J, Schubert K. Microstructure grooves with a width of less than 50 μm cut with ground hard metal micro end mills. *Precis Eng* 1999;23:229–35.
- [22] Dornfeld DA, Lee DE. *Precision manufacturing*. New York: Springer-Verlag; 2008.